Nanostructures

DOI: 10.1002/ange.201001931

Monodisperse Gold–Copper Bimetallic Nanocubes: Facile One-Step Synthesis with Controllable Size and Composition**

Yonglin Liu and A. R. Hight Walker*

Gold and gold-containing alloy nanocrystals (NCs) with cubic morphologies have extraordinary crystalline structure and plasmonic properties, which facilitate multiple applications.[1–4] For instance, cubic gold (or Au–Ag alloy) nanocages are promising candidates for nanoreactors used in photocatalysis,[1] and for many biomedical applications.[2–7] In general, monodisperse cubic NCs are of great interest as building blocks for self-assembly, a significant step towards the controlled design of novel nanostructured materials and devices.[8–10] Gold nanocubes have been produced using a variety of techniques, such as seed-mediated methods,[11–13] electrochemical techniques,[14] and polyol methods,[15,16] whilst gold-containing alloy NCs with cubic morphologies have been produced only by galvanic replacement reactions.[17] To make greater progress with the above applications, a facile, reliable synthetic procedure in terms of better productivity, monodispersity, and cube shape and size control is still highly desirable. Furthermore, whilst sub-10 nm NCs showed significant improvements in activity and selectivity compared to their larger counterparts,[18–21] there is no previous reported synthesis of sub-10 nm gold or gold-containing NCs with cubic morphologies in solution. This lack of success is partially due to the fact that controlling the shape of the NCs is a kinetically controlled process, not a thermodynamically controlled one; thus, adjustment of any synthetic parameter to reduce the size can also lead to a change in shape.[16] Moreover, recent studies by Dovgolevsky and Haick[12] suggested that it is unlikely that gold nanocubes less than 25 nm in length can be produced in solution owing to the large average surface self-diffusion distance of gold (3 nm–12 nm).[22] Herein, we report that such barriers can be overcome by alloying gold with other metals, such as copper.

[*] Dr. Y. Liu, Dr. A. R. H. Walker
Optical Technology Division, Physics Laboratory
National Institute of Standards and Technology
Gaithersburg, MD 20899-8443 (USA)
E-mail: yonglin.liu@nist.gov

[**] Certain commercial equipment, instruments, or materials are identified in this paper to foster understanding and does not imply recommendation or endorsement by NIST, nor does it imply that the materials or equipment identified are necessarily the best available for the purpose. Y.L. acknowledges the support of the National Research Council (NRC, NIH(NIBIB)/NIST) for a research associate fellowship. Both authors acknowledge the Maryland NanoCenter and its NispLab (the NispLab is supported in part by the NSF as a MRSEC Shared Experimental Facility), the University of Maryland X-ray crystallographic center, and Dr. Zhufang Liu for XRD measurements.

Supporting information for this article is available on the WWW under http://dx.doi.org/10.1002/anie.201001931.

The physicochemical properties of NCs are often determined, and can therefore be tuned by, their size, shape, and composition, among other parameters.[2,16,23,24] For instance, cubic NCs have a significant advantage over spherical ones in terms of self-assembly,[25,26] repeatable hot spots for surface-enhanced Raman scattering (SERS),[27] and other applications.[28] Also, bimetallic gold–copper alloy NCs with tunable sizes and compositions provide wider control over their plasmon properties than single metallic NCs.[29] The ability to engineer size, morphology, and composition is also of great interest to the Nano Environmental, Health, and Safety (EHS) community, as isolation of these parameters prior to toxicological testing is necessary to understand their true impact.[30] Thus, the synthesis of gold–copper nanocubes of controllable length (especially ≤ 10 nm) is a significant and worthwhile task, both synthetically and practically. Nevertheless, the growth of bimetallic NCs, such as gold–copper structures, appears to be much more difficult owing to complications in the solution phase[31] and because of the tendency of self-purification.[32,33] Gold–copper bimetallic nanoparticles have been produced in several cases in the absence of morphological control.[34–37] Most recently, rod-shaped gold–copper NCs were produced using a seed-mediated protocol.[29] Although computational studies revealed the possible existence of gold–copper nanocubes,[31,38,39] to the best of our knowledge, there has yet to be a report on the solution preparation of gold–copper bimetallic nanocubes. Herein, we report a facile, one-step colloidal polyol method for the synthesis of uniform, single-crystalline gold–copper nanocubes with controllable size and composition.

The gold–copper nanocubes were synthesized by the simultaneous reduction of copper(II) acetylacetonate, [Cu(acac)$_2$], and gold chloride ($HAuCl_4$) by 1,2-hexadecanediol (HDD) in diphenyl ether (DPE) solvent, which also contained 1-adamantanecarboxylic acid (ACA), 1-hexadecylamine (HDA), and 1-dodecanethiol (DDT). A typical transmission electron microscopy (TEM) image of the nanocubes is shown in Figure 1a. The as-prepared particles are perfectly cubic in shape and substantially uniform in size, averaging (22.9 ± 2.4) nm (Figure 1b). The nanocubes shown in Figure 1a were prepared using a high-speed centrifuge (16 krpm), without the size-separation process used for nanoparticles in some previous reports.[11,15] Thus, it is convincing that monodisperse gold–copper nanocubes have been produced from this polyol process. The TEM diffraction pattern (Figure 1c) shows a face-centered cubic (fcc) structure consistent with a single-phase gold–copper alloy. In the energy-dispersive X-ray spectroscopy (EDX) line-scanning analysis, the compositional line profiles of copper and gold

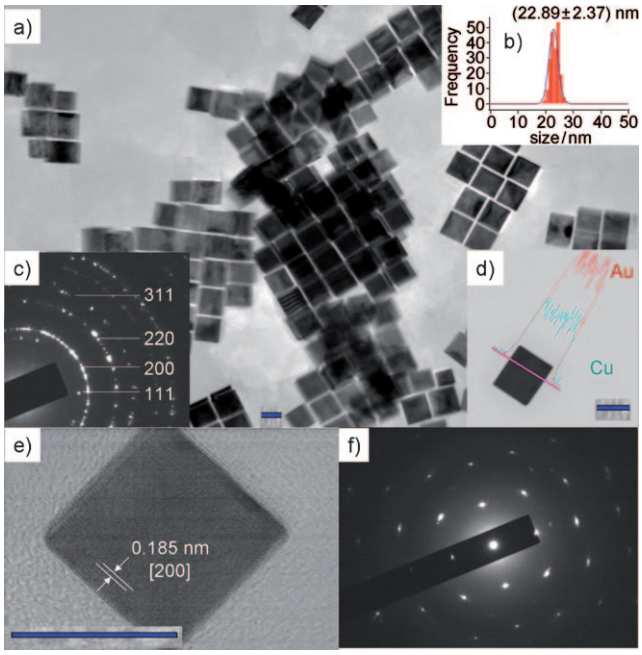

Figure 1. a) TEM image of $AuCu_3$ nanocubes with an average edge length of 22.9 nm; the reaction was conducted at 180 °C with $HAuCl_4$/$[Cu(acac)_2]$/DDT in a molar ratio of 1:3:25. b) Histogram represents the measurement of 200 nanocubes. c) TEM diffraction pattern of the as-prepared nanocubes. d) STEM image and the corresponding EDX spectra following a line-scanning profile of a single nanocube. e) HRTEM image and f) SAED pattern of a single nanocube. The scale bars represent 20 nm.

indicate that the nanocubes are a homogeneous gold–copper alloy without any segregation, showing an approximate atomic ratio of 3:1 (Cu/Au; Figure 1d). The high-resolution TEM (HR-TEM) analysis (Figure 1e) and the selected-area electron diffraction (SAED) pattern (Figure 1f) of a typical nanocube support the single-crystalline nature of the as-prepared nanocubes. The visible lattice fringes corresponded to a spacing of 0.185 nm, which matched well with the expected *d*-spacing (0.187 nm) of the (200) plane of the $AuCu_3$ alloy.

To better understand the formation mechanism of the nanocubes, we monitored their production process by withdrawing samples at different times along the synthesis. Figure 2a–d shows TEM images of samples taken from the reaction solution at 1 hour, 1.5 hours, 5 hours, and 24 hours, respectively. At 1 hour, the gold–copper nanocubes were observed along with cuboctahedral and polyhedral NCs; the nanocubes, averaging (8.7 ± 2.3) nm in edge length, were slightly truncated. The average diameter of the cuboctahedral shape is (6.7 ± 1.7) nm, whilst that of polyhedral NCs was as small as 4–5 nm. Both cuboctahedral and polyhedral NCs are intermediate stages in the formation of nanocubes.[12,40,41] At 1.5 hours and 5 hours, only nanocubes were detected, averaging (15.7 ± 2.4) nm and (22.9 ± 2.4) nm, respectively (Figure 2b and 2c). The nanocubes observed at 5 hours had a narrower size distribution than those at 1.5 hours. At this stage, smaller nanocubes grow into large ones with edge-sharpening and size-focusing, presumably by Ostwald ripening.[15,42] After 24 hours (Figure 2d), the size of the nanocubes remained similar to that observed after 5 hours, thus indicating that the cube formation was complete at approximately 5 hours.

The role of each component in our synthetic procedure was then investigated. The co-existence of DDT, $[Cu(acac)_2]$, and $HAuCl_4$ in the starting solution was a prerequisite for the formation of gold–copper alloy nanocubes. DDT acted as a co-reducing agent by accelerating the reduction rate of copper(II) and decreasing that of gold(III), consistent with previous reports.[43] Support for this postulation can be seen in the different decomposition behaviors of copper and gold precursors. In the absence of DDT, $[Cu(acac)_2]$ decomposes into copper NCs after being heated at 180 °C for 12 h,[44] whilst $HAuCl_4$ decomposes into gold NCs at 80 °C. In comparison, gold–copper nanocubes start to form within one hour at 180 °C in the presence of DDT. DDT also plays a critical role in the morphology control of nanocubes. In the absence of DDT, for instance, we observed multiple twinned NCs along

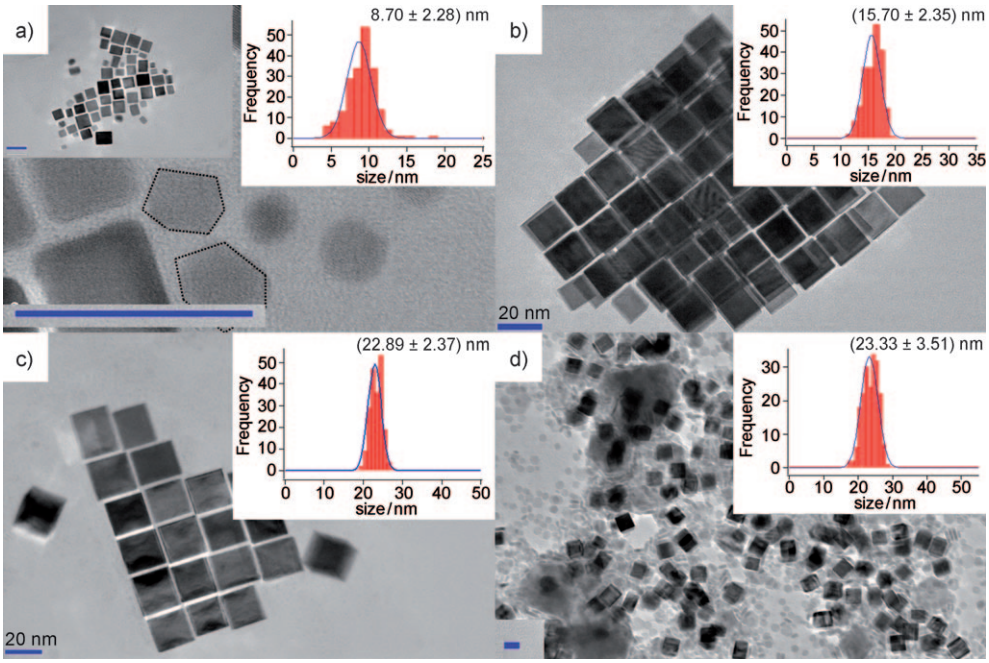

Figure 2. TEM images of nanoparticles collected at different reaction times during the synthesis of 22.9 nm $AuCu_3$ nanocubes: a) 1 h, b) 1.5 h, c) 5 h, and 24 h. Insets: the corresponding histograms showing the measurements of 200 nanocrystals. The scale bars represent 20 nm.

with small numbers of truncated nanocubes (ca. 5%; see the Supporting Information, Figure S2).

The control experiment in the absence of $[Cu(acac)_2]$ led to the formation of gold NCs with irregular shapes (see the Supporting Information, Figure S3). The reaction of a 1:10 molar ratio of $[Cu(acac)_2]/HAuCl_4$ starts to produce nanocubes with a size of 5–50 nm, along with large branched nanostructures (see the Supporting Information, Figure S4). These branched nanostructures are presumably generated from the aggregation of small NCs with insufficient surface protection. Performing the reaction with a 12:1 molar ratio of $[Cu(acac)_2]/HAuCl_4$ exclusively afforded nanocubes with a size of 2–20 nm (see the Supporting Information, Figure S5). These observations indicate that $[Cu(acac)_2]$ is not only one of the reactants, but also an important surface protecting agent for nanocubes. Note that the reaction using $CuCl_2$ instead of $[Cu(acac)_2]$ also produced nanocubes (see the Supporting Information, Figure S6), thus indicating that the acetylacetonate group does not play an effective role in the reaction. This observation is consistent with the previous report of Cu^{2+} ions acting as an effective agent for controlling gold nanostructures.[45] In addition, our previous studies showed that hexagonal Cu_2S nanoplates are produced under similar conditions in the absence of $HAuCl_4$,[44] thus indicating that $HAuCl_4$ is necessary for nanocube formation.

The edge length of gold–copper nanocubes can be rationally controlled by varying the amounts of DDT, $[Cu(acac)_2]$, and $HAuCl_4$ in the starting solution. For example, by keeping the amounts of DDT (0.5 mL) and $HAuCl_4$ (26 mg) constant but increasing the amount of $[Cu(acac)_2]$ to 98 mg, gold–copper nanocubes with a size of 45 nm were produced (Figure 3a and 3b). These perfect nanocubes are monodispersed, averaging (44.9 ± 4.7) nm. Both the HRTEM image (Figure 3d) and an SAED pattern (Figure 3e) of one typical cube revealed that they are single-crystalline, with the interfringe distance measured to be 0.188 nm, close to the (200) planes at 0.187 nm in the face-centered cubic $AuCu_3$ alloy crystal. Addition of 130 mg of $[Cu(acac)_2]$ whilst keeping the other experimental parameters the same led to the formation gold–copper nanocubes with a size of 85 nm (see the Supporting Information, Figure S7).

The most significant challenge is to produce monodisperse nanocubes with lengths below 10 nm. We found that this can be easily achieved by decreasing the amount of $[Cu(acac)_2]$ and DDT in the starting solution. For instance, using 26 mg of $HAuCl_4$, 8 mg of $[Cu(acac)_2]$, and 0.1 mL of DDT, gold–copper nanocubes below 10 nm in length were produced. The as-prepared NCs are exclusively perfectly cubic, with a uniform edge length of 5 nm ((5.0 ± 0.7) nm; Figure 4a, also see the Supporting Information, Figure S8). To the best of our knowledge, this success represents the first synthesis of monodisperse gold–copper nanocubes with a size of 5 nm. Further characterization using TEM diffraction (Figure 4b), HRTEM of one individual nanocube (Figure 4c, inset), and fast Fourier transform (FFT; Figure 4c, inset), showed that each nanocube is composed of an fcc alloy of $AuCu_3$ and appeared to be single-crystalline bound by (200) facets. The composition of gold–copper alloy nanocubes was further confirmed by STEM of one nanocube in conjunction with

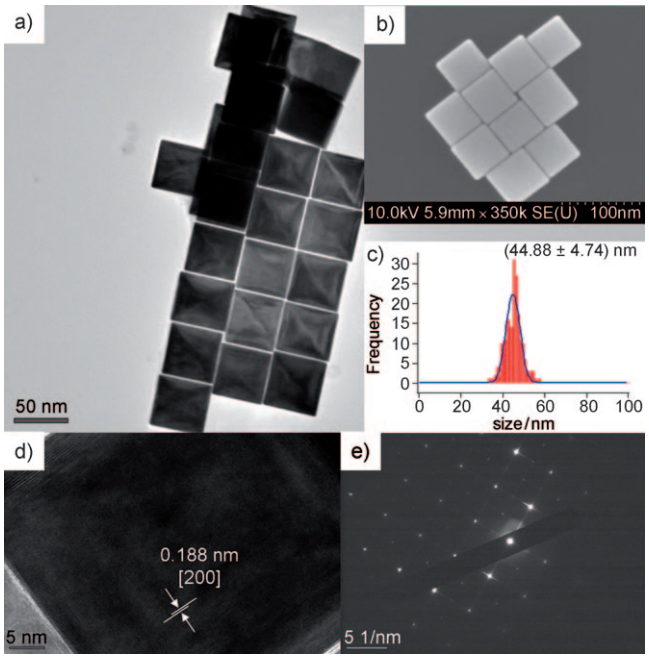

Figure 3. a) TEM image of 44.9 nm $AuCu_3$ nanocubes. The reaction was conducted at 180°C. The molar ratio of $HAuCl_4/[Cu(acac)_2]$/DDT was 1:5:25. b) SEM and c) histogram showing 200 measurements of the as-prepared nanocubes. d) HRTEM image and e) SAED pattern of a single nanocube.

EDX line profiling analysis (Figure 4d), which showed a homogeneous distribution of copper and gold across the entire nanocube. Notice that the formation reaction of 5 nm nanocubes happened much faster (ca. 20 min) than that of the 23 nm nanocubes (ca. 5 h). This observation indicates that it is a kinetically controlled process. Furthermore, the amount of $HAuCl_4$ plays a critical role in the production of monodisperse 5 nm nanocubes. The control reaction, by reducing the amount of $HAuCl_4$ to 4 mg, led to the formation of NCs with various morphologies and size distribution (see the Supporting Information, Figure S9). Therefore, we believe that the excess $HAuCl_4$ (or AuCl) plays at least two important roles during the formation of 5 nm nanocubes: First, it acts as a surface-protecting agent for the 5 nm nanocubes. Second, the excess amount of $HAuCl_4$ in the starting solution also restricts the formation of noncubic NCs. An attempt to produce monodisperse nanocubes by further decreasing the amount of $[Cu(acac)_2]$ failed. As mentioned above, the reaction with a significant excess of $HAuCl_4$ (50 mg) to $[Cu(acac)_2]$ (5 mg) led to branched nanostructures larger than 500 nm along with small amounts of nanocubes (see the Supporting Information, Figure S4). These branched nanostructures are presumably formed by the aggregation of small NCs in the absence of enough surface stabilization by Cu^{2+} ions.

In addition to DDT, $[Cu(acac)_2]$, and $HAuCl_4$ the formation of monodisperse nanocubes also depends on HDD. As a mild reducing agent, diols containing long carbon chains (such as HDD) can assist the nucleation process.[43] In the absence of HDD, we did not observe any nanocrystal formation after 5–10 hours, though previous reports[46,47] have stated that HDA or DDT alone can reduce

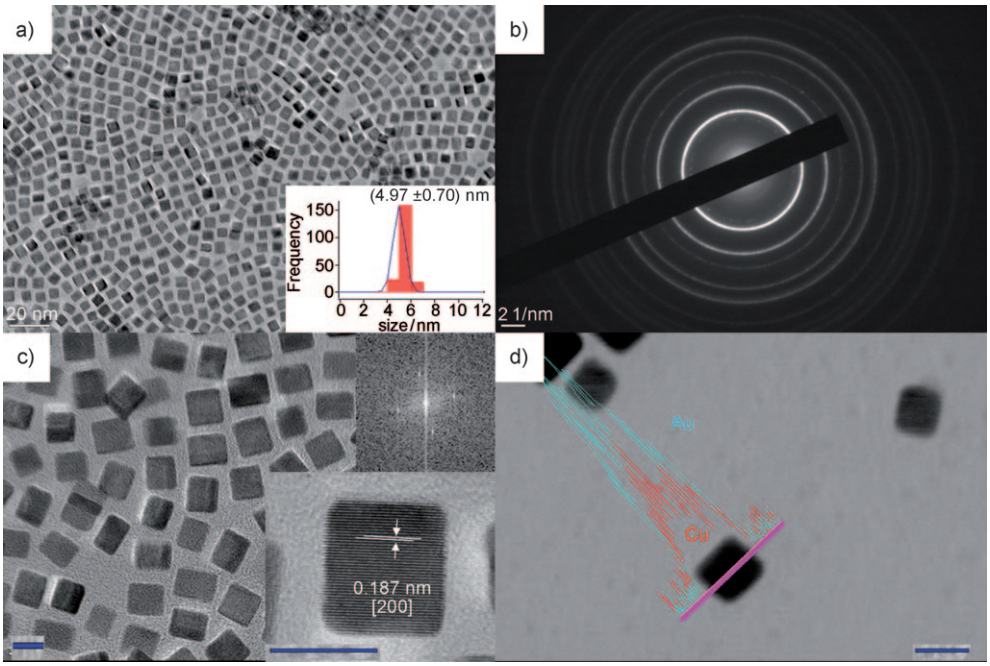

Figure 4. a) TEM image of 4.97 nm $AuCu_3$ nanocubes. The molar ratio of $HAuCl_4$/[Cu(acac)$_2$]/DDT was 1:0.4:5. Inset: the histogram showing 200 measurements of the as-prepared nanocubes. b) TEM diffraction pattern and c) HRTEM of as-prepared nanocubes. Inset: the HRTEM image of a single nanocube (bottom) and its corresponding FFT pattern (top). d) STEM image and the corresponding EDX spectra following a line-scanning profile of a single nanocube. The unmarked scale bars represent 5 nm.

metal ions into NCs. Furthermore, we found that the length of carbon chain of the diol also played an important role during the formation of nanocubes. For instance, the reaction using hexanediol did not lead to the formation of nanoparticles, whilst using 1,2-dodecanediol (DDD) instead of HDD led to the formation of branched NCs with only 5% nanocubes (see the Supporting Information, Figure S10). This observation suggests that HDD, which has the same length carbon chain as HDA, also acted as a surface-protecting agent during the formation of monodisperse nanocubes. It has been previously reported that under relatively low concentrations of HDD, bimetallic nanorods or octapod nanostructures were produced.[48] The concentration of HDD was decreased five times to study its effect on the shape of the gold–copper NCs. Surprisingly, instead of nanorods and octapods, nanocubes with even smaller sizes were obtained (see the Supporting Information, Figure S11a). The monodisperse single-crystalline nanocubes, averaging (3.4 ± 0.6) nm, were further assigned to a $AuCu_3$ fcc alloy on the basis of the HRTEM analysis (see the Supporting Information, Figure S11b) and the TEM diffraction pattern (see the Supporting Information, Figure S11c). One-step production of perfect gold–copper nanocubes of sub-10 nm length is the most significant feature of this synthesis; nanocubes of 3.4 nm represent an even more remarkable achievement and may hold great potential in various fields.

Our investigation on the functions of the two remaining components showed that ACA played a critical role in forming the sharp edges of the nanocubes (see the Supporting Information, Figure S12a), whilst HDA is an important factor in maintaining the uniformity of the nanocubes (see the Supporting Information, Figure S12b). Furthermore, purging the reaction mixture with argon was not necessary for the formation of nanocubes (see the Supporting Information, Figure S13), and polar solvents favored nanocube formation, likely owing to charged surfaces of Cu^{2+} as we proposed earlier(see the Supporting Information, Figure S14b).

This procedure for synthesizing nanocubes of controllable size combined with the nature of the gold–copper alloy enabled us to further adjust the nanostructure composition while maintaining the cubic morphology. For instance, using 100 mg of $HAuCl_4$, 65 mg of [Cu(acac)$_2$], and 0.5 mL of DDT afforded gold–copper nanocubes of 5 nm (see the Supporting Information, Figure S15 and Figure S16). However, the composition of these nanocubes was determined to be fcc single-crystalline Au_3Cu alloys on the basis of TEM (see the Supporting Information, Figure S15b), HRTEM (Figure S15c), FFT of a single cube (Figure S15b, inset), and EDX analysis (Figure S15d). Moreover, as with $AuCu_3$ nanocubes, the sizes of the Au_3Cu structures could be adjusted. For instance, by decreasing the amount of $HAuCl_4$ to 85 mg whilst maintaining the amount of DDT (0.5 mL) and [Cu(acac)$_2$] (65 mg), Au_3Cu nanocubes of 12 nm in length were observed (see the Supporting Information, Figure S17).

Surface plasmon resonance (SPR) wavelength strongly depends on the nanocrystal composition, morphology, and size.[29,49] To the best of our knowledge, optical absorption spectra of gold–copper nanocubes have not been reported. As shown in the Supporting Information, Figure S18, the UV/Vis/NIR spectra of the colloidal suspensions of each of the five different-sized nanocubes exhibited one broad SPR band. This single SPR band for all of these nanocubes indicated the formation of a single metallic nanocrystalline phase, thus confirming our TEM observations. A similar observation was previous reported for spherical gold–copper NCs.[34] Furthermore, the SPR bands of as-prepared gold–copper nanocubes are highly dependent upon the size of the nanocubes. The 3.4, 5, 23, 45, and 85 nm diameter nanocubes displayed SPR bands of 529, 553, 599, 625, and 659 nm, respectively, showing a red shift with increasing size of the nanocubes. This observation can also be seen in the notable color changes of the corresponding solutions from pink, to purple, blue, dark brown, and dark blue, respectively (see the Supporting

Information, Figure S18, inset). On the basis of previous studies, $AuCu_3$ NCs showed a SPR band closer to that of copper NCs with similar morphologies.[34] Our data appear to be consistent with this observation. For instance, 100 nm nanocubes of gold and copper show SPR bands at 593 nm[15] and 610 nm[50], respectively, compared with our observation of 659 nm for 85 nm nanocubes.

In summary, a one-pot polyol strategy for the synthesis of gold–copper nanocubes has been developed. This represents the first production of gold–copper bimetallic nanocubes, as confirmed by multiple physicochemical characterization methods. By carefully adjusting the reaction parameters, not only the edge length of the resulting nanocubes was controlled to form 3.4 nm, 5 nm, 23 nm, 45 nm, and 85 nm nanocubes, but also the composition could be varied from $AuCu_3$ to Au_3Cu.

Received: March 31, 2010
Revised: June 16, 2010
Published online: August 16, 2010

Keywords: alloys · copper · gold · nanocubes · nanostructures

[1] C. W. Yen, M. A. Mahmoud, M. A. El-Sayed, *J. Phys. Chem. A* **2009**, *113*, 4340.
[2] S. E. Skrabalak, J. Y. Chen, Y. G. Sun, X. M. Lu, L. Au, C. M. Cobley, Y. N. Xia, *Acc. Chem. Res.* **2008**, *41*, 1587.
[3] J. Chen, F. Saeki, B. J. Wiley, H. Cang, M. J. Cobb, Z. Y. Li, L. Au, H. Zhang, M. B. Kimmey, X. D. Li, Y. Xia, *Nano Lett.* **2005**, *5*, 473.
[4] H. Cang, T. Sun, Z. Y. Li, J. Y. Chen, B. J. Wiley, Y. N. Xia, X. D. Li, *Opt. Lett.* **2005**, *30*, 3048.
[5] X. M. Yang, S. E. Skrabalak, Z. Y. Li, Y. N. Xia, L. H. V. Wang, *Nano Lett.* **2007**, *7*, 3798.
[6] J. Y. Chen, B. Wiley, Z. Y. Li, D. Campbell, F. Saeki, H. Cang, L. Au, J. Lee, X. D. Li, Y. N. Xia, *Adv. Mater.* **2005**, *17*, 2255.
[7] J. Y. Chen, D. L. Wang, J. F. Xi, L. Au, A. Siekkinen, A. Warsen, Z. Y. Li, H. Zhang, Y. N. Xia, X. D. Li, *Nano Lett.* **2007**, *7*, 1318.
[8] A. Ahniyaz, Y. Sakamoto, L. Bergstrom, *Proc. Natl. Acad. Sci. USA* **2007**, *104*, 17570.
[9] M. Chen, J. Kim, J. P. Liu, H. Y. Fan, S. H. Sun, *J. Am. Chem. Soc.* **2006**, *128*, 7132.
[10] T. Ming, X. S. Kou, H. J. Chen, T. Wang, H. L. Tam, K. W. Cheah, J. Y. Chen, J. F. Wang, *Angew. Chem.* **2008**, *120*, 9831; *Angew. Chem. Int. Ed.* **2008**, *47*, 9685.
[11] T. K. Sau, C. J. Murphy, *J. Am. Chem. Soc.* **2004**, *126*, 8648.
[12] E. Dovgolevsky, H. Haick, *Small* **2008**, *4*, 2059.
[13] W. X. Niu, S. L. Zheng, D. W. Wang, X. Q. Liu, H. J. Li, S. A. Han, J. Chen, Z. Y. Tang, G. B. Xu, *J. Am. Chem. Soc.* **2009**, *131*, 697.
[14] C. J. Huang, P. H. Chiu, Y. H. Wang, W. R. Chen, T. H. Meen, *J. Electrochem. Soc.* **2006**, *153*, D129.
[15] D. Seo, J. C. Park, H. Song, *J. Am. Chem. Soc.* **2006**, *128*, 14863.
[16] A. R. Tao, S. Habas, P. D. Yang, *Small* **2008**, *4*, 310.
[17] Y. G. Sun, Y. N. Xia, *Science* **2002**, *298*, 2176.
[18] W. Tang, H. F. Lin, A. Kleiman-Shwarsctein, G. D. Stucky, E. W. McFarland, *J. Phys. Chem. C* **2008**, *112*, 10515.
[19] P. Kalimuthu, S. A. John, *J. Electroanal. Chem.* **2008**, *617*, 164.
[20] C. K. Tsung, J. N. Kuhn, W. Y. Huang, C. Aliaga, L. I. Hung, G. A. Somorjai, P. D. Yang, *J. Am. Chem. Soc.* **2009**, *131*, 5816.
[21] J. N. Kuhn, W. Y. Huang, C. K. Tsung, Y. W. Zhang, G. A. Somorjai, *J. Am. Chem. Soc.* **2008**, *130*, 14026.
[22] C. Alonso, R. C. Salvarezza, J. M. Vara, A. J. Arvia, L. Vazquez, A. Bartolome, A. M. Baro, *J. Electrochem. Soc.* **1990**, *137*, 2161.
[23] Y. Xia, Y. J. Xiong, B. Lim, S. E. Skrabalak, *Angew. Chem.* **2009**, *121*, 62; *Angew. Chem. Int. Ed.* **2009**, *48*, 60.
[24] N. Tian, Z. Y. Zhou, S. G. Sun, Y. Ding, Z. L. Wang, *Science* **2007**, *316*, 732.
[25] F. Li, S. A. Delo, A. Stein, *Angew. Chem.* **2007**, *119*, 6786; *Angew. Chem. Int. Ed.* **2007**, *46*, 6666.
[26] H. J. Chen, Z. H. Sun, W. H. Ni, K. C. Woo, H. Q. Lin, L. D. Sun, C. H. Yan, J. F. Wang, *Small* **2009**, *5*, 2111.
[27] P. H. C. Camargo, M. Rycenga, L. Au, Y. N. Xia, *Angew. Chem.* **2009**, *121*, 2214; *Angew. Chem. Int. Ed.* **2009**, *48*, 2180.
[28] J. Hernandez, J. Solla-Gullon, E. Herrero, A. Aldaz, J. M. Feliu, *J. Phys. Chem. C* **2007**, *111*, 14078.
[29] A. Henkel, A. Jakab, G. Brunklaus, C. Sonnichsen, *J. Phys. Chem. C* **2009**, *113*, 2200.
[30] D. R. Boverhof, R. M. David, *Anal. Bioanal. Chem.* **2010**, *396*, 953.
[31] R. Ferrando, J. Jellinek, R. L. Johnston, *Chem. Rev.* **2008**, *108*, 845.
[32] D. J. Norris, A. L. Efros, S. C. Erwin, *Science* **2008**, *319*, 1776.
[33] G. M. Dalpian, J. R. Chelikowsky, *Phys. Rev. Lett.* **2006**, *96*, 226802.
[34] A. K. Sra, T. D. Ewers, R. E. Schaak, *Chem. Mater.* **2005**, *17*, 758.
[35] A. K. Sra, R. E. Schaak, *J. Am. Chem. Soc.* **2004**, *126*, 6667.
[36] R. E. Schaak, A. K. Sra, B. M. Leonard, R. E. Cable, J. C. Bauer, Y. F. Han, J. Means, W. Teizer, Y. Vasquez, E. S. Funck, *J. Am. Chem. Soc.* **2005**, *127*, 3506.
[37] W. Chen, R. Yu, L. Li, A. Wang, Q. Peng, Y. Li, *Angew. Chem.* **2010**, *122*, 2979; *Angew. Chem. Int. Ed.* **2010**, *49*, 2917.
[38] W. H. Qi, B. Y. Huang, M. P. Wang, *Physica B* **2009**, *404*, 1761.
[39] N. T. Wilson, R. L. Johnston, *J. Mater. Chem.* **2002**, *12*, 2913.
[40] D. Kim, N. Lee, M. Park, B. H. Kim, K. An, T. Hyeon, *J. Am. Chem. Soc.* **2009**, *131*, 454.
[41] J. T. Ren, R. D. Tilley, *J. Am. Chem. Soc.* **2007**, *129*, 3287.
[42] T. K. N. Hoang, L. Deriemaeker, V. B. La, R. Finsy, *Langmuir* **2004**, *20*, 8966.
[43] D. Xu, Z. P. Liu, H. Z. Yang, Q. S. Liu, J. Zhang, J. Y. Fang, S. Z. Zou, K. Sun, *Angew. Chem.* **2009**, *121*, 4281; *Angew. Chem. Int. Ed.* **2009**, *48*, 4217.
[44] Y. Liu, A. R. Hight Walker, *J. Phys. Chem. C* **2010**, *114*, 4264.
[45] J. H. Sun, M. Y. Guan, T. M. Shang, C. L. Gao, Z. Xu, J. M. Zhu, *Cryst. Growth Des.* **2008**, *8*, 906.
[46] D. A. Fleming, M. E. Williams, *Langmuir* **2004**, *20*, 3021.
[47] S. Panigrahi, S. Kundu, S. Basu, S. Praharaj, S. Jana, S. Pande, S. K. Ghosh, A. Pal, T. Pal, *J. Phys. Chem. C* **2007**, *111*, 1612.
[48] Q. S. Liu, Z. Yan, N. L. Henderson, J. C. Bauer, D. W. Goodman, J. D. Batteas, R. E. Schaak, *J. Am. Chem. Soc.* **2009**, *131*, 5720.
[49] S. W. Prescott, P. Mulvaney, *J. Appl. Phys.* **2006**, *99*, 123504.
[50] Y. H. Wang, P. L. Chen, M. H. Liu, *Nanotechnology* **2006**, *17*, 6000.

